(Preprint) AAS XX-XXX

PROPAGATION OF PERIODIC AND QUASIPERIODIC ORBITS USING THE HARMONIC BALANCE METHOD

Nicolas Leclère, Gaëtan Kerschen*

The harmonic balance method (HBM) is a well-known method to compute periodic solutions of nonlinear systems in the frequency domain. The extension of HBM to multiple frequencies for the computation of quasiperiodic solutions is the multi-harmonic balance method (MHBM). Their applications to the field of orbital propagation provide a simple and efficient alternative to the usual time domain integration. When combined with Hill's method, HBM also comes with a straightforward approach to evaluate the Floquet multipliers, which indicate stability loss and the presence of bifurcations. This study proposes the application of HBM and MHBM to the classic circular restricted 3-body problem (CRTBP) and the case of the asteroid 433 Eros.

INTRODUCTION

Celestial mechanics has always fascinated and stimulated mankind, it began with Sir Isaac Newton in 1687 who formulated the laws of universal gravitation and Kepler who wrote his famous three laws few years before that. These equations laid down a strong basis for the study of orbital propagation, from simple problem such as the circular restricted three-body problem (CRTBP) to the exploration of irregular celestial bodies such as asteroids. The first to prove the existence of periodic orbits in the CRTBP is Poincaré.[1] With the rise of computer power and the evolution of numerical methods, the search for periodic solutions grew rapidly. Multiple numerical studies improved the general idea of the existence of families of periodic orbits around equilibrium points,[2,3].[4] The most recent studies were focused on the study of bifurcations around the equilibrium points.[5] A complete map of periodic orbits near the collinear equilibrium points connected to the triangular points was proposed by Doedel.[6] With the usage of multiple Poincaré sections[7] computed quasiperiodic orbits in the Sun-Earth system. While the CRTBP remains a topic of great interest by its simple aspect but still relevant for real applications, the focus on the exploration of small irregular bodies kept on growing for the last decades. They are not only considered as echoes of the early state of the universe, and thus are extremely important to better understand the origin of space, but they are also a potential *fuel station* for long distance explotation missions. This was the goal of some of the recent JAXA and NASA missions such as the Hayabusa I and II or the Osiris Rex that impacted asteroids to bring back samples to Earth.[8] The study of the celestial rocks is also important to estimate how to act in the eventuality of a collision with Earth. The DART mission was designed around the objective to impact and deflect the Dimorphos moon of asteroid 65803-Didymos.[9] The irregular shape of asteroids affects the motion of a spacecraft that would orbit around it. This is the reason why numerous analytical and numerical methods have been considered to model the potential as accurately as possible. Three in particular stand out, the approximation of the shape

*Space Structures and Systems Laboratory, University of Liège, Liège, Belgium

of the asteroid with triaxial ellipsoid or spherical harmonics,[10],[11] the mascon (mass concentration) method where the potential of an asteroid is simulated by different masses grouped together,[12].[13] The third method, based on radar observations or *in situ* topography, is the polyhedron method for which a surface mesh is built and a constant density is assumed,[14].[15] The search of periodic orbits in this context is important to build multiple orbit paths that can respond to various mission goals. A grid-searching method was proposed to detect periodic orbits around Kleopatra with the polyhedron method.[16] This method despite being costly computation-wise was applied to different asteroids to compute periodic orbits,[17],[18].[19] The approach presented in this paper is the Harmonic Balance method (HB), which consists in rewritting the equations in order to compute periodic solutions in the frequency domain rather than the time domain. The orbit and the nonlinear forces are approximated by truncated Fourier series. Usually the method is applied to mechanical systems for vibration analysis such as a Duffing oscillator but also to more complex structures,[20].[21] Combined with Hill's method, the Floquet multipliers and the stability of the orbits are easily estimated.[22] The coefficients also provide information about the different types of bifurcations.[23] An extension of the classical HB method based on a multi Fourier decomposition exists and allows the computation of quasiperiodic solutions.[24] The method was successfully applied to complex structures,[25].[26] This work presents the application of the HB method and its extension to the case of the circular restricted three body problem and the case of the asteroid 433 Eros. The stability is adressed and the search for bifurcations is also achieved. The results obtained are an extension of a previous work.[27]

ORBITAL PROPAGATION

Circular restricted three-body problem

The circular restricted three-body problem (CRTBP) is a simplification of the general three-body system where the motion of a small body with respect to two larger bodies is studied. The assumptions of the CRTBP are that this third body has an infinitesimal mass (m_3) compared to the two main bodies, also called primaries (m_1 and m_2). The two primaries have a circular motion around the barycenter of the system, thus the distance between the two primaries remain constant. Main perturbations such as atmospheric drag or solar radiation pressure are neglected. The motion of m_3 with respect to the two primaries is described by adimensionalized Newton's Law of gravity corresponding to Eq.(1)[28]

$$\begin{cases} \ddot{x} - 2\dot{y} - x = -(1-\mu)(x+\mu)\, r_1^{-3} - \mu(x-1+\mu)\, r_2^{-3} \\ \ddot{y} + 2\dot{x} - y = -(1-\mu)\, y r_1^{-3} - \mu y r_2^{-3} \\ \ddot{z} = -(1-\mu)\, z r_1^{-3} - \mu z r_2^{-3} \end{cases} \tag{1}$$

where μ is the mass ratio $m_2/(m_1+m_2)$. In this paper, we set $\mu = 0.012155085$ which is the mass ratio in the Earth-Moon system. r_1 and r_2 are the distances between the third body and the two primaries, respectively.

$$r_1 = \sqrt{(x+\mu)^2 + y^2} \tag{2}$$

$$r_2 = \sqrt{(x-1+\mu)^2 + y^2} \tag{3}$$

Lagrangian Points

This system has a total of five equilibrium points, known as the Lagrange points or libration points. They are the result of a balance between the centrifugal force and the gravitational attraction of the primaries. Three of them, L_1, L_2 and L_3, are collinear and their position can be obtained by solving the simplified Eq.1 where the velocity and acceleration are set to zero:

$$\begin{cases} x - (1-\mu)(x+\mu)\, r_1^{-3} - \mu\,(x-1+\mu)\, r_2^{-3} = 0 \\ y = 0 \end{cases} \tag{4}$$

while the two remaining points, L_4 and L_5, are called equilateral points since their positions are determined under the constraint $r_1 = r_2$. For the Earth-Moon system studied in this paper the Lagrange points adimensionalized positions are gathered in Table 1.[29]

	L_1	L_2	L_3	L_4	L_5
x	0.83689	1.15569	-1.00506	0.48784	0.48784
y	0	0	0	$\frac{\sqrt{3}}{2}$	$-\frac{\sqrt{3}}{2}$

Table 1: Position of the Lagrange points for the Earth-Moon CRTBP with $\mu = 0.012155085$

These points are important since families of periodic orbits emanate from them.[6] An orbit $\mathbf{X}(t)$ is periodic of period T if $\mathbf{X}(t) = \mathbf{X}(t+T)$.

Jacobi constant

The CRTBP has only one conserved quantity called the Jacobi constant. The three equations of the system Eq.1 are respectively multiplied by $\dot{x}$, $\dot{y}$, and $\dot{z}$ and added together such that the new derivative equation is obtained:

$$\ddot{x}\dot{x} + \ddot{y}\dot{y} + \ddot{z}\dot{z} = \dot{x}\Omega_x + \dot{y}\Omega_y + \dot{z}\Omega_z \tag{5}$$

where the indices $_x$, $_y$ and $_z$ stand for the derivative with respect to x, y and z. Ω is the pseudo-potential such that:

$$\begin{cases} \Omega_x = x - (1-\mu)(x+\mu)\, r_1^{-3} - \mu\,(x-1+\mu)\, r_2^{-3} \\ \Omega_y = y - (1-\mu)\, y r_1^{-3} - \mu y r_2^{-3} \\ \Omega_z = -(1-\mu)\, z r_1^{-3} - \mu z r_2^{-3}. \end{cases} \tag{6}$$

The time integration of Eq.5 gives the explicit expression of the Jacobi constant, C.

$$\dot{x}^2 + \dot{y}^2 + \dot{z}^2 = 2\Omega - C \tag{7}$$

Eq.7 is reorganized such that the velocity, V, is made apparent.

$$C = 2\Omega - V^2 \tag{8}$$

The physical interpretation of this constant is associated to the accessible region of a spacecraft. Since this value is conserved for a given orbit, its value constraints the third mass motion. Thus forbidden regions exist depending on the value of the Jacobi constant, and are defined as a region that cannot be reached by the third mass due to its initial conditions. Since the Jacobi constant remains unchanged for a given periodic orbit, it is a great tool to compare orbits with each others.

Irregular celestial bodies

In the particular case of an irregularly shaped body the equations of motion in a rotating frame that rotates at a constant angular velocity ω_a take the form:

$$\ddot{\mathbf{x}} + 2\omega_{\mathbf{a}} \times \dot{\mathbf{x}} + \omega_{\mathbf{a}} \times (\omega_{\mathbf{a}} \times \mathbf{x}) + \nabla U(\mathbf{x}) = 0 \tag{9}$$

The body-fixed vector that links the asteroid body's center of mass to the particle is denoted $\mathbf{x}$, the determination of the potential of a three-dimensional body, $U(\mathbf{x})$, with the polyhedron method was presented by.[14] It is a geometric method based on a surface mesh of an asteroid where the density is assumed uniform. The equation takes the form

$$U(\mathbf{x}) = \frac{1}{2} G\rho \sum_{edges} (\mathbf{r}_e \cdot \mathbf{E}_e \cdot \mathbf{r}_e) \cdot L_e - \frac{1}{2} G\rho \sum_{faces} (\mathbf{r}_f \cdot \mathbf{F}_f \cdot \mathbf{r}_f) \cdot \omega_f \tag{10}$$

where ρ is the bulk density of the body, G is the gravitational constant, the two vectors $\mathbf{r}_e$ and $\mathbf{r}_f$ are body-fixed vectors from the particle to the edge e and the face f, respectively. Matrices $\mathbf{E}_e$ and $\mathbf{F}_f$ gather the geometric parameters of the edges e and faces f. $\mathbf{L}_e$ denotes the integration factor of the particle position and the edge e whereas ω_f corresponds to the solid angle of the face f relative to the particle. The Gradient and the Laplacian can easily be derived from Eq. 10

$$\nabla U(\mathbf{x}) = -G\rho \sum_{edges} (\mathbf{E}_e \cdot \mathbf{r}_e) \cdot L_e + G\rho \sum_{faces} (\mathbf{F}_f \cdot \mathbf{r}_f) \cdot \omega_f \tag{11}$$

$$\nabla^2 U(\mathbf{x}) = -G\rho \sum_{faces} \omega_f \tag{12}$$

In order to determine if the field point orbiting an asteroid collides with it, the Laplacian of the potential is a great tool. If the point is outside of the polyhedron model the sum $\sum_{faces} \omega_f$ vanishes, when the point is inside the polyhedron model the sum is equal to 4π. Its simple expression makes it ideal to detect collisions.

In the rotating frame of the asteroid, the Jacobi constant takes the form

$$J = \frac{1}{2}\dot{\mathbf{x}} \cdot \dot{\mathbf{x}} - \frac{1}{2}(\omega_a \times \mathbf{x}) \cdot (\omega_a \times \mathbf{x}) + U(x) \tag{13}$$

The Near Earth Asteroid Rendezvous Mission (NEAR) has for goal to study one of the largest near-Earth asteroids, 433 Eros. The probe Shoemaker closely orbited the asteroid for over a year taking multiple pictures of the celestial rock which allowed to build an accurate polyhedron mesh to

numerically reproduce Eros. The highly irregular shape as well as the fact that Eros is a near-Earth asteroid make it an ideal candidate to work with. In the scope of this paper, only the asteroid 433 Eros is studied but the method can easily be extended to additional asteroids. The polyhedron model that consists of 1708 faces and 856 edges is shown in Fig. 1.

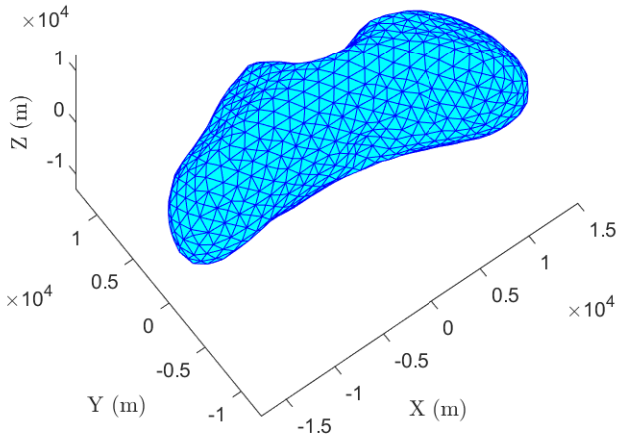

Figure 1: Polyhedron model 3D of 433 Eros with 1708 faces.

METHOD

Harmonic balance method

The method considered in the scope of this paper to compute periodic orbits is the Harmonic balance method. The position over time $x(t)$ is appoximated by a Fourier serie truncated to the N_H-th harmonic:

$$x(t) = \frac{c_0^x}{\sqrt{2}} + \sum_{k=1}^{N_H} \left(s_k^x \sin(k\omega t) + c_k^x \cos(k\omega t)\right) \tag{14}$$

A similar decomposition is carried out for the nonlinear forces, for the two cases studied in this paper it corresponds to the right part of Eq.1 for the CRTBP and ∇U for an asteroid.

$$f_{nl} = \frac{c_0^f}{\sqrt{2}} + \sum_{k=1}^{N_H} \left(s_k^f \sin(k\omega t) + c_k^f \cos(k\omega t)\right) \tag{15}$$

Vectors s_k and c_k are the Fourier coefficients associated to the sine and cosine, respectively. ω is the frequency of the periodic orbit (which is not correlated to the angular velocity of the asteroid, ω_a). The Fourier coefficients are gathered in a new vector $\mathbf{z}$ for the displacement and $\mathbf{b}$ for the nonlinear force of dimension $(2N_H + 1)\, n \times 1$, with n the degrees of freedom of the studied system, $n = 3$ in this present case.

$$\mathbf{z} = \begin{bmatrix} c_0^x & s_1^x & c_1^x & \cdots & s_{N_H}^x & c_{N_H}^x \end{bmatrix}^T \tag{16}$$

$$\mathbf{b} = \begin{bmatrix} c_0^f & s_1^f & c_1^f & \cdots & s_{N_H}^f & c_{N_H}^f \end{bmatrix}^T \tag{17}$$

Eq.16 and Eq.17 are recast in a more compact expression[30]

$$\mathbf{x}(t) = (\mathbf{Q}(t) \otimes I_n)\, \mathbf{z} \tag{18}$$

$$\mathbf{f}_{nl}(t) = (\mathbf{Q}(t) \otimes I_n)\, \mathbf{b} \tag{19}$$

the symbol $\otimes$ stands for the Kronecker tensor product and I_n is the identity matrix of size n. The vector $\mathbf{Q}$ corresponds to the sine and cosine of the Fourier decomposition. Eq. 18 can easily be derived with respect to time to obtain an expression of the velocity and the acceleration in the same compact form.

$$\dot{\mathbf{x}}(t) = \left(\dot{\mathbf{Q}}(t) \otimes I_n\right) \mathbf{z} \tag{20}$$

$$\ddot{\mathbf{x}}(t) = \left(\ddot{\mathbf{Q}}(t) \otimes I_n\right) \mathbf{z} \tag{21}$$

The property of the Kronecker tensor product that $(\mathbf{A} \otimes \mathbf{B})\,(\mathbf{C} \otimes \mathbf{D}) = (\mathbf{AC}) \otimes (\mathbf{BD})$ allows the rewritting of Eq. 9 with respect to $\mathbf{z}$ and $\mathbf{b}$

$$\left(\ddot{\mathbf{Q}}(t) \otimes I_n\right) \mathbf{z} + \left(\dot{\mathbf{Q}}(t) \otimes \mathbf{C}\right) \mathbf{z} + (\mathbf{Q}(t) \otimes \mathbf{K})\, \mathbf{z} - (\mathbf{Q}(t) \otimes I_n)\, \mathbf{b} = 0 \tag{22}$$

with the matrices $\mathbf{C} = \begin{bmatrix} 0 & -2\omega_a & 0 \\ 2\omega_a & 0 & 0 \\ 0 & 0 & 0 \end{bmatrix}$ and $\mathbf{K} = \begin{bmatrix} -\omega_a^2 & 0 & 0 \\ 0 & -\omega_a^2 & 0 \\ 0 & 0 & 0 \end{bmatrix}$ in the particular case of an asteroid described by Eq.9, the matrix asociated to the mass is simply I_n. The time dependency of Eq. 22 can be removed by the projection on the orthogonal trigonometric basis $\mathbf{Q}(t)$ with a Galerkin procedure[20] such that the equations of motion are recast in their final and more compact form

$$\mathbf{h}(\mathbf{z}, \omega) = \mathbf{A}(\omega)\mathbf{z} - \mathbf{b}(\mathbf{z}) = \mathbf{0} \tag{23}$$

The matrix $\mathbf{A}$ describes the linear dynamics. Eq 23 is solved iteratively with a Newton-Raphson procedure. The continuation is ensured with a predictor-corrector algorithm, such as a tangent prediction and a corrector based on the Moore-Penrose corrections. This approach presents numerous advantages over the classical time integration method. Working in the frequency domain provides a fast and efficient alternative from time domain methods to solve the equations of motion.

Due to the time-invariant form of Eq.1 and Eq.9, it is mandatory to impose a phase condition to insure the uniqueness of the periodic solution. If $x(t)$ is a solution, $x(t + \Delta t)$ is a solution as well for any Δt.[31] The simplest phase condition is to set one of the unknowns to 0, in classical time domain method that would be the initial position or velocity of one of the degrees of freedom. In the frequency domain the condition is simply to imposed a Fourier coefficient equal to zero.

Stability & bifurcations

In the time domain, the stability of orbits, as well as the detection of bifurcations, is determined through the eigenvalues of the monodromy matrix also known as Floquet multipliers or exponents.[32] If the magnitude of at least one of the Floquer multiplier is higher than 1, the orbit is unstable. In the frequency domain, an alternative method known as Hill's method exists[22] to approximate the Floquet multipliers. It consists in introducing the periodic solution $\mathbf{x}^*(t)$ perturbed with another periodic solution $\mathbf{s}(t)$ modulated by an exponential decay into the equation of motion, Eq. 9

$$\mathbf{p}(t) = \mathbf{x}^*(t) + e^{\lambda t}\mathbf{s}(t) \tag{24}$$

which eventually leads to the simple quadratic eigenvalue problem[33]

$$\left(\Delta_2\lambda^2 + \Delta_1\lambda + \mathbf{h_z}\right)\mathbf{u} = \mathbf{0} \tag{25}$$

with $\Delta_2 = \begin{bmatrix} \mathbf{C} & & & & & \\ & \mathbf{C} & -2\omega I_n & & & \\ & 2\omega I_n & \mathbf{C} & & & \\ & & & \ddots & & \\ & & & & \mathbf{C} & -2N_H\omega I_n \\ & & & & 2N_H\omega I_n & \mathbf{C} \end{bmatrix}$, $\Delta_1 = I_{2N_H+1} \otimes I_n$ and $\mathbf{h_z}$ being the Jacobian with respect to the Fourier coefficient $\mathbf{z}$. The $(2N_H + 1)\,2n$ eigenvalues obtained via this method do not have all physical meaning and are for the most part spurious. According to,[34] only the $2n$ eigenvalues with the smallest imaginary part in modulus are to be considered. An efficient sorting method for the eigenvalues of the hill's method was recently presented by[35]

It is worth mentioning that for autonomous systems such as the orbital propagation studied in the scope of this paper, 2 out of the $2n$ Floquet multipliers are always equal to 1. This is due to the trivial singularity of $\mathbf{h_z}$. Since the HB method is based on a Fourier decomposition, the amount of harmonics, N_H, is responsible for the precision degree of the solution. The null eigenvalues prevent accurate computation of the stability or bifurcations points. In order to improve the results, the zero eigenvalues can be shifted to a negative value.[36]

There are four different types of bifurcation that can be detected thanks to the Floquet theory for periodic orbits around celestial bodies.[37] Tangent bifurcations, period-doubling bifurcations, real saddle bifurcations, and Neimark-Sacker bifurcations.[38]

Tangent bifurcation A tangent bifurcation is characterized by Floquet multipliers leaving or joining the unit circle along the real axis through +1 or in other words Floquet exponents $\lambda = 0$. Those bifurcations are also known as singular bifurcations since at the bifurcation point the Jacobian matrix $\mathbf{h_z}$ is singular. Therefore, a detection of the bifurcation is to evaluate the determinant of $\mathbf{h_z}$ when its value is 0 there is a tangent bifurcation.

Among the tangent bifurcations, two types of tangent bifurcations can be identified. The fold, or limit points, bifurcation and the branch point. The first one corresponds to the collision of two

solutions stable and unstable. No additional branches arise for this bifurcation. The second one corresponds to a change of stability followed by the creation of new branches of solution. The uniqueness of the solution is lost. Two types of branch points are possible, either the curve of solutions loops back on itself and the branch point is called a transcritical bifurcation or the symmetry of the system is broken[39] and a new branch symmetric with respect to the main branch is created. In order to distinguish the fold from the branch points the Jacobian with respect to the frequency $\mathbf{h}_\omega$ is used. For a fold,

$$\mathbf{h}_\omega \notin \text{range}\left(\mathbf{h}_\mathbf{z}\right) \tag{26}$$

while for a branch point the bifurcation verifies

$$\mathbf{h}_\omega \in \text{range}\left(\mathbf{h}_\mathbf{z}\right) \tag{27}$$

In other words, if the extended Jacobian $[\mathbf{h}_\mathbf{z}, \mathbf{h}_\omega]$ removes the singularity of the Jacobian the bifurcation is a limit point, otherwise it is a branch point. The singularity of the matrix can be monitored via its rank. If the rank of the matrix changes from $n\left(2N_H+1\right)-1$ to $n\left(2N_H+1\right)$ the singularity is removed.

Period-Doubling bifurcations Period-doubling bifurcations are characterized by a pair of Floquet multipliers leaving or entering the unit circle along the real axis through -1. From this bifurcation a new branch of solution also emerges. The solutions also are periodic but with a period of $2T$ compared to a period of T for the solutions of the initial branch.

Neimark-Sacker bifurcations When the Floquet multipliers leave or enter the unit circle as complex conjugates the resulting bifurcation is a Neimark-Sacker bifurcation. This type of bifurcation induces the creation of a new branch of quasi-periodic solutions. Quasi-periodic solutions depend on at least two different frequencies, the main one ω and a second one ω_2. The ratio of the two frequencies is irrational. A quite good first approximation for ω_2 is to use the absolute value of the imaginary part of the pair of the Floquet exponents associated to the bifurcation.

Real Saddle bifurcations Real saddle bifurcations are associated to Floquet multipliers joining or leaving the real axis. This kind of bifurcations is not often discussed in the literature. The only few references of it can be found in.[38]

Figure 2 is a graphical representation of the different behaviors of the Floquet multipliers for the different bifurcations.

Multi-Harmonic balance method

The HB method is limited to the evaluation of periodic orbits due to the nature of the Fourier decomposition. However, it can easily be extended to compute quasiperiodic solutions if a multiple Fourier series approximates the position and the nonlinear force. This method is known as the Multi-Harmonic balance method (MHBM). The series is constructed on a frequency basis of size $M \geq 2$

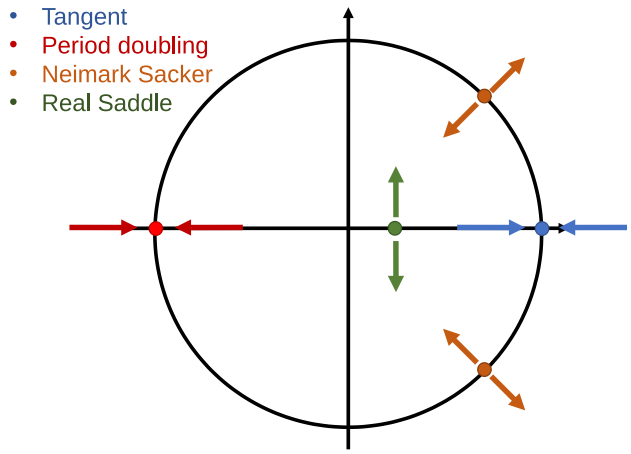

Figure 2: Evolution of the Floquet multipliers for the four different types of bifurcations on a unit circle.

$$x(t) = \sum_{\mathbf{k} \in Z^M}^{N_{H_M}} \left(s_k^x \sin((\mathbf{k}, \boldsymbol{\omega})t) + c_k^x \cos((\mathbf{k}, \boldsymbol{\omega})t) \right) \tag{28}$$

$$f_{nl} = \sum_{\mathbf{k} \in Z^M}^{N_{H_M}} \left(s_k^f \sin((\mathbf{k}, \boldsymbol{\omega})t) + c_k^f \cos((\mathbf{k}, \boldsymbol{\omega})t) \right) \tag{29}$$

where $\boldsymbol{\omega}$ is now a vector of frequency basis, $\boldsymbol{\omega} = [\omega_1, \cdots, \omega_M]^T$, $\mathbf{k}$ is a vector of the harmonic indexes and $(,)$ corresponds to the scalar product such that $(\mathbf{k}, \boldsymbol{\omega})t = \sum_{j=1}^{M} k_j \omega_j t$.[25] The concept of hypertime, $\boldsymbol{\tau} = \boldsymbol{\omega} t$ is introduced in order to manage such functions. Each component of τ contains 2π in classical time.

For instance the relation between the classical time and the hyper time gives

$$\dot{\mathbf{x}} = \frac{\partial \mathbf{x}}{\partial t} = \frac{\partial u}{\partial t} \frac{\partial \boldsymbol{\tau}}{\partial t} = \frac{\partial \tilde{\mathbf{x}}}{\partial t} \boldsymbol{\omega}. \tag{30}$$

The MHBM follows the same procedure as the classical HBM, a predictor corrector algorithm, however the dimensions of the matrices are considerably larger which increases the computational cost.

RESULTS

Application to the circular restricted three-body problem

The application of the HB method to the CRTBP around the equilibrium points allows the computation of well-known orbit families, in particular in the vicinity of the first Lagrange points. Fig.3 shows the evolution of the Jacobi constant of the periodic orbits obtained via the HB method with respect to their adimensionalized period. Four different families are identified, the $L1$ Lyapunov family depicted in red, which consists of in-plane orbits that share two branch point bifurcations with the axial family $A1$, in yellow, and the halo family $H1$, in blue. Both are out-of-plane evolution of the Lyapunov family. The symmetry of the system means that those two families have a symetrical counterpart, the $H1$ family can either grow to the positive Z-axis (North) or the negative Z-axis (South). The $A1$ family can shift to the left or to the right until it eventually reaches a vertical position that leads to another branch point to merge with the vertical family $V1$ represented by the green color. These results only correspond to a part of the continuation process focused on the bifurcation, the continuation could be pursued until the orbit and one of the main bodies collide. Fig.4 is a graphical representation of a sampled orbit of each of the four families. A more detailed figure of each family is given in Fig.5 to 8 where the bifurcations are highlighted in the same color as the orbits on Fig4. Obviously, these results are not bounded to the first Lagrange point and the method can be extended to the other equilibrium points.

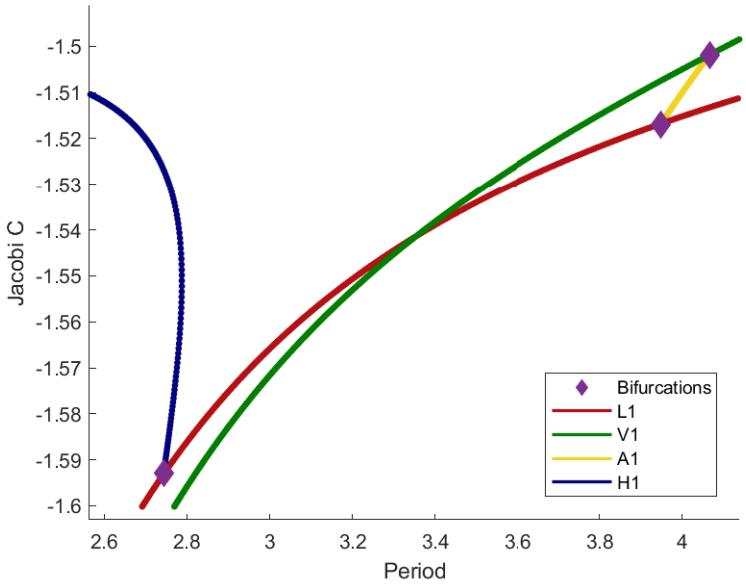

Figure 3: Bifurcation diagram of periodic orbits around the first Lagrange point in the CRTBP for the Earth-Moon system.

Looking at the Floquet multipliers for those families shows that these orbits are unstable since there is at least one of the 6 multipliers that is greater than one for all the orbits. All the bifurcations displayed on Fig.3 are branch points, which means that 2 of the multipliers are converging to +1. Since 2 additional multipliers are always equal to +1 for the periodic orbits in the CRTBP, only the 2 lasts multipliers provide information for the stability at the bifurcations. Their values are gathered

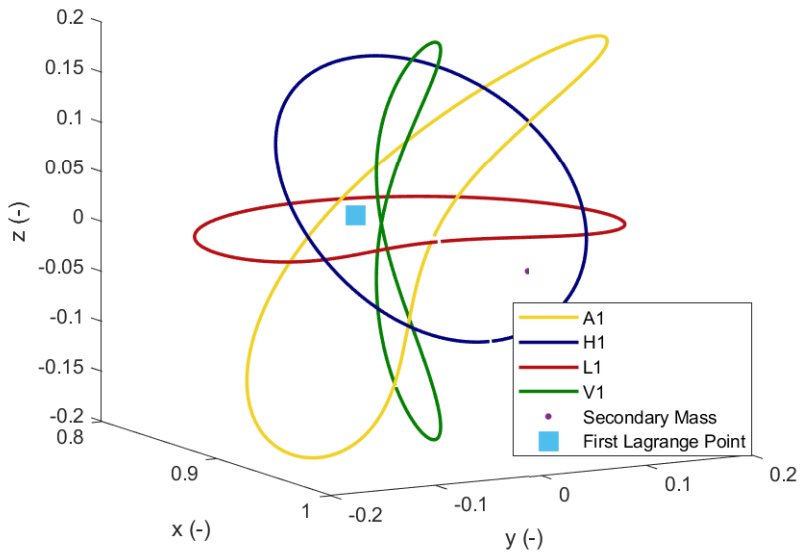

Figure 4: Representation of sampled orbits of the four periodic orbit families around the first Lagrange point.

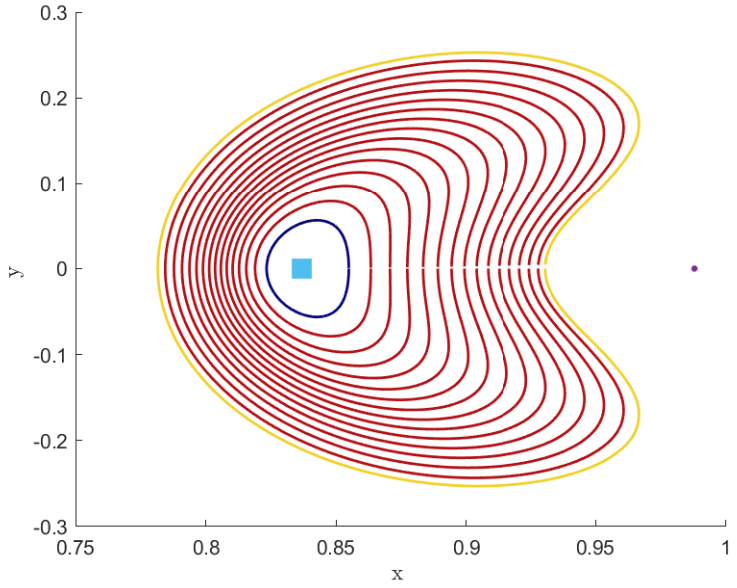

Figure 5: Continuation of the L1 family.

in Table 2.

Despite the existence of quasi-periodic orbits in the CRTBP such as the Lissajous or the quasi-Halo orbits the MHBM did not manage to capture them. It could be that the quasi-periodic orbits in the CRTBP have more than two frequencies entangled together or that the MHBM solutions are

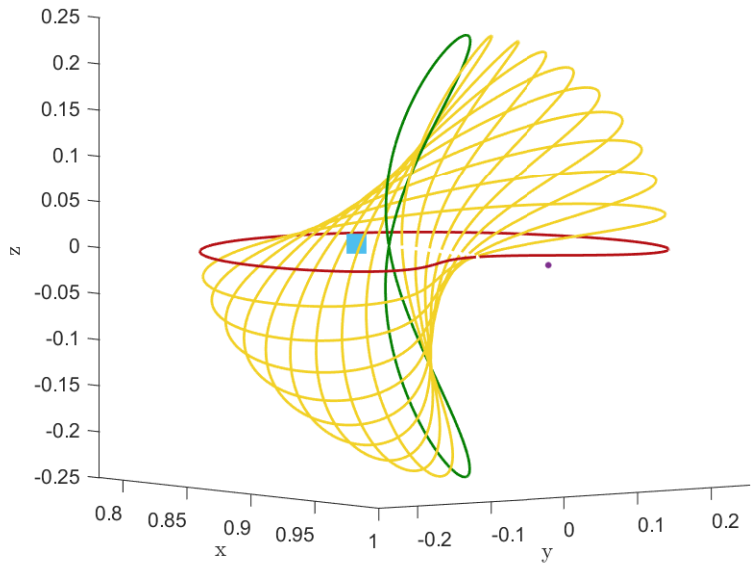

Figure 6: Continuation of the A1 family.

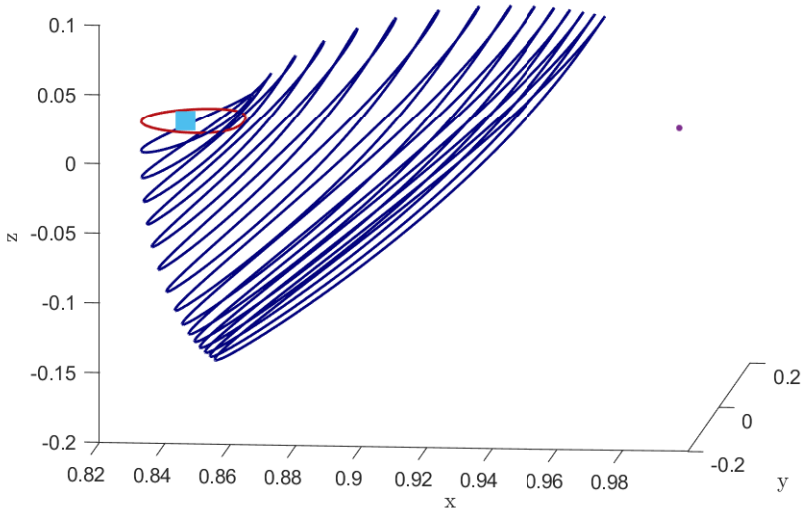

Figure 7: Continuation of the H1 family.

either the results of a quasi-periodic excitation or quasi-periodic orbits emanating from a Neimarck-Sacker bifurcation.

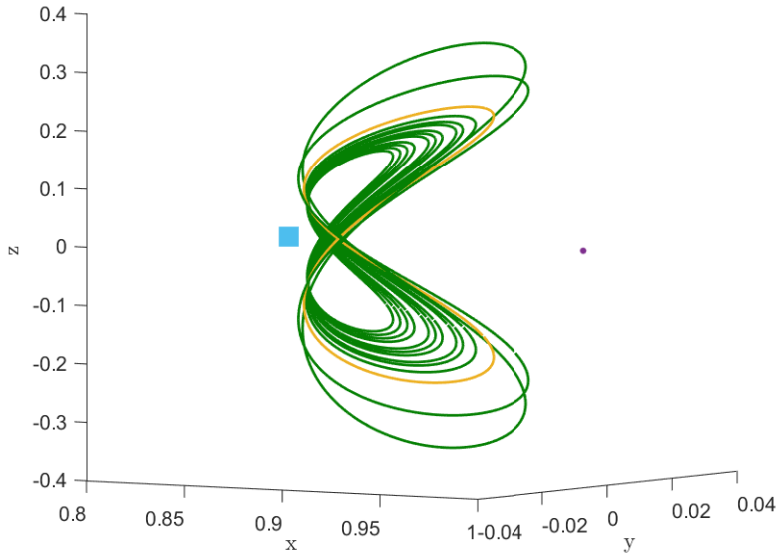

Figure 8: Continuation of the V1 family.

	$L1$-$H1$	$L1$-$A1$	$V1$-$A1$
λ_1	0.00044628	0.002467	0.001966
λ_2	2240.716030	405.277616	508.734835

Table 2: Real part of the Floquet multipliers at the bifurcations in the case of the CRTBP.

433 Eros

This section concerns the application of HBM and MHBM to compute periodic and quasi-periodic orbits around the asteroid 433 Eros. The continuation is achieved between a periodic ratio, ω/ω_a of 0.5 up to 3. Figure 9 represents the evolution of the Jacobi constant over that range for periodic orbits, stable orbits are depicted in black while unstable orbits are red. The four types of bifurcations are encountered numerous times. The tangent bifurcations correspond to the circles, the period doubling bifurcations to the squares, the real saddle bifurcations to the diamonds and the Neimark Sacker to the small stars. In total 38 bifurcations are detected, the period ratio, the Jacobi constant and the type of bifurcation are gathered in Table 3. This list is non-exhaustive since more periodic orbits might exist in the vinicity of Eros that could lead to more bifurcations. The HBM is based on an Fourier series truncated to the N_{th} harmonic, meaning that complex periodic orbits requiring a high amount of harmonics to be computed can be missed for the sake of computational efficiency. Several observations can be made about Fig.9, first most of the stable orbits are found for lower period ratio. It mainly consists in orbits with a simple circular shape and that are further away from the asteroid than the ones with higher periodic ratio. Thus, the irregularity of the gravity potential due to the asteroid shape have less impact on the orbits. However, a small unstable region bounded by two period doubling bifurcations is detected around $\omega/\omega_a = 0.56$. Secondly, the importance of resonances is well apparent. The Jacobi constant, which is the general energy integral of the system, varies the most around the period ratio 1:1 2:1 and 3:1. Most of the bifurcations

are also located around these specific period ratio. In particular around $\omega/\omega_a = 2$, Fig.10 shows a close up near the resonance. In total, 25 bifurcations are listed on this small window, most of them are grouped in pair at almost similar period ratio and Jacobi constant. This is directly correlated to the close symmetry of the orbits, that share almost similar shape but the irregularity of the gravity potential induces differences in the shape of the orbits and the associated bifurcations. In 2018,[40] introduced the concept of *pseudo-bifurcations* around the asteroid 22 Kalliope, and in particular period doubling bifurcations appearing around the half integer periodic ratio. This phenomenon can also be observed in Fig.9 where period doubling bifurcations are detected near the period ratio 1.5:1 and 2.5:1. A sample of periodic orbits can be found in the appendix. The application of the MHBM near the two Neimark-Sacker bifurcations detected, (n°23 and n°25 in Table2) allows the computation of quasiperiodic orbits. On Fig.12 and Fig.11, the orbits (yellow) clearly exhibit quasiperiodic oscillations around the associated periodic solutions (red) found at the bifurcations.

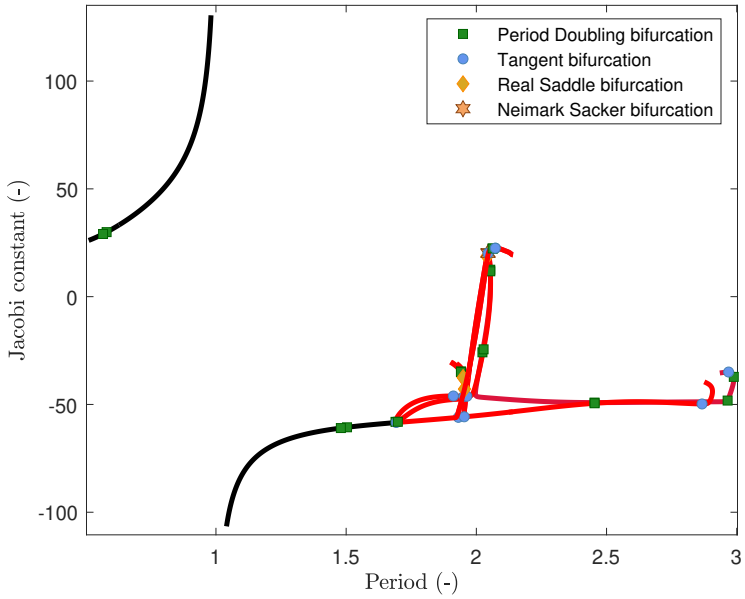

Figure 9: Piecewise continuation of periodic orbits around 433 Eros.

CONCLUSIONS

This work presents a new approach for the computation of periodic orbits for the CRTBP and around asteroids. The HB method offers an easy and efficient way to detect bifurcations and compute the stability of periodic orbits. The importance of resonances have been highlighted. For the first time, the multiple HBM was applied to orbital propagation. For the first time, quasiperiodic orbits around 433 Eros have been found emerging from a Neimarck-Sacker bifurcation with MHBM.

REFERENCES

[1] H. Poincaré, *Les méthodes nouvelles de la mécanique céleste.* Gauthier-Villars, 1892.

[2] T. Chanut, S. Aljbaae, and V. Carruba, "Numerical determination of short-period trojan orbits in the restricted three-body problem," *The Astronomical journal*, Vol. 71, No. 2, 1965.

Bifurcation n°	Period ratio	Jacobian constant	Bifurcation
1	0.56636	29.06982	Period Doubling
2	0.58015	29.93583	Period Doubling
3	1.47968	-60.95185	Period Doubling
4	1.50336	-60.59228	Period Doubling
5	1.68957	-58.07696	Period Doubling
6	1.69232	-58.36660	Tangent
7	1.69849	-58.05187	Period Doubling
8	1.91178	-46.08617	Tangent
9	1.93094	-55.98424	Tangent
10	1.9408	-34.96881	Period Doubling
11	1.9409	-34.65819	Period Doubling
12	1.9491	-37.52710	Real Saddle
13	1.9501	-37.57214	Real Saddle
14	1.95229	-46.16384	Tangent
15	1.95428	-42.95244	Real Saddle
16	1.95454	-42.77661	Real Saddle
17	1.95353	-55.72538	Tangent
18	1.96362	-46.20752	Tangent
19	2.02338	-25.82402	Period Doubling
20	2.02784	-24.42617	Period Doubling
21	2.04085	18.689559	Real Saddle
22	2.04092	18.678435	Real Saddle
23	2.0446	20.081901	Neimark Sacker
24	2.0449	20.090995	Tangent
25	2.0450	20.394694	Neimark Sacker
26	2.0455	20.410718	Tangent
27	2.05347	12.503698	Period Doubling
28	2.05360	11.755616	Period Doubling
29	2.06253	22.347709	Period Doubling
30	2.06257	22.311943	Period Doubling
31	2.07265	22.491516	Tangent
32	2.07381	22.451597	Tangent
33	2.45382	-49.13622	Period Doubling
34	2.45419	-49.45353	Period Doubling
35	2.86677	-49.77554	Tangent
36	2.9650	-48.19868	Period Doubling
37	2.9687	-34.96828	Tangent
38	2.9887	-37.21302	Period Doubling

Table 3: Bifurcations, stability and period ratio of the orbit families

[3] T. Bray and C. Goudas, "Doubly symmetric orbits about the collinear Lagrangian points," *The Astronomical journal*, Vol. 72, No. 2, 1966.

[4] V. Szbehely and E. Grebenikov, "Theory of orbits - The restricted problem of three bodies," *Soviet Astronomy*, Vol. 13, No. 2, 1968, https://doi.org/10.1016/B978-0-12-395732-0.50007-6.

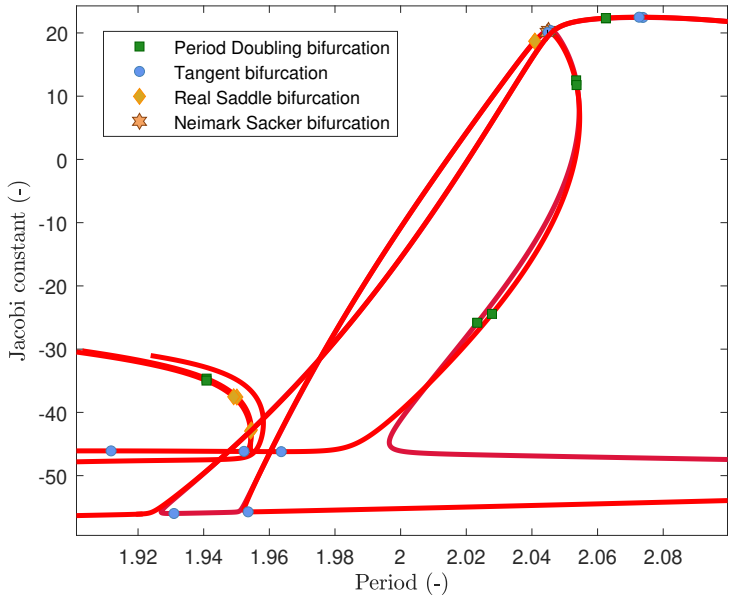

Figure 10: Zoom around the resonance 2:1 on the continuation of periodic orbits around 433 Eros.

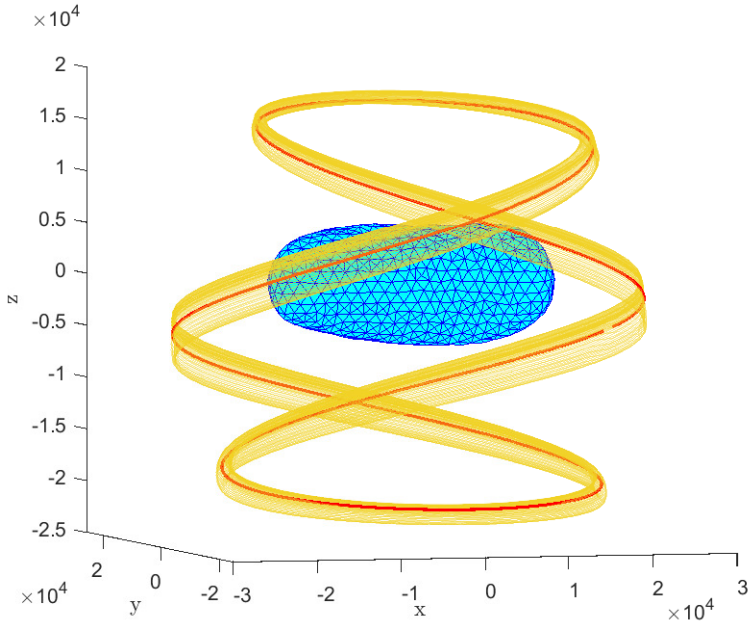

Figure 11: Quasiperiodic (yellow) and periodic (red) orbits around 433 Eros emerging from bifurcation n°23.

[5] K. Papadakis and C. Zagouras, "Bifurcation points and intersection of families of periodic orbits in the three-dimensional restricted three-body problem," *Astrophysics and Space Science*, Vol. 199, No. 2, 1968.

[6] E. Doedel, R. Paffenroth, H. Keller, D. Dichmann, J. Galan-Vioque, and A. Vanderbauwhede, "Elemental periodic orbits associated with the libration points in the circular restricted 3-body problem,"

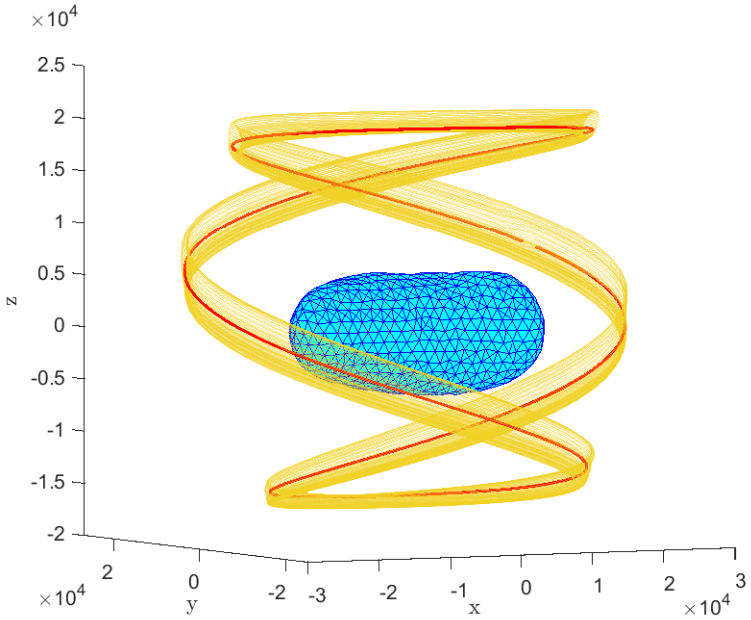

Figure 12: Quasiperiodic (yellow) and periodic (red) orbits around 433 Eros emerging from bifurcation n°25.

International Journal of Bifurcation and Chaos, Vol. 17, May 2006, 10.1142/S0218127407018671.

[7] E. Kolemen, N. J. Kasdin, and P. Gurfil, "Quasi-Periodic Orbits of the Restricted Three-Body Problem Made Easy," *AIP Conference Proceedings*, Vol. 886, 02 2007, pp. 68–77, 10.1063/1.2710044.

[8] Y. Tsuda, M. Yoshikawa, M. Abe, H. Minamino, and S. Nakazawa, "System design of the Hayabusa 2—Asteroid sample return mission to 1999 JU3," *Acta Astronautica*, Vol. 91, 2013, pp. 356–362, https://doi.org/10.1016/j.actaastro.2013.06.028.

[9] A. F. Cheng, A. S. Rivkin, P. Michel, J. Atchison, O. Barnouin, L. Benner, N. L. Chabot, C. Ernst, E. G. Fahnestock, M. Kueppers, P. Pravec, E. Rainey, D. C. Richardson, A. M. Stickle, and C. Thomas, "AIDA DART asteroid deflection test: Planetary defense and science objectives," *Planetary and Space Science*, Vol. 157, 2018, pp. 104–115, https://doi.org/10.1016/j.pss.2018.02.015.

[10] D. Scheeres, "Dynamics about Uniformly Rotating Triaxial Ellipsoids: Applications to Asteroids," *Icarus*, Vol. 110, No. 2, 1994, pp. 225–238, https://doi.org/10.1006/icar.1994.1118.

[11] J. Sebera, A. Bezděk, I. Pešek, and T. Henych, "Spheroidal models of the exterior gravitational field of Asteroids Bennu and Castalia," *Icarus*, Vol. 272, 2016, pp. 70–79, https://doi.org/10.1016/j.icarus.2016.02.038.

[12] T. G. G. Chanut, S. Aljbaae, and V. Carruba, "Mascon gravitation model using a shaped polyhedral source," *Monthly Notices of the Royal Astronomical Society*, Vol. 450, 05 2015, pp. 3742–3749, 10.1093/mnras/stv845.

[13] P. T. Wittick and R. P. Russell, "Mixed-model gravity representations for small celestial bodies using mascons and spherical harmonics," *Celestial Mechanics and Dynamical Astronomy*, Vol. 131, No. 7, 2019, 10.1007/s10569-019-9904-6.

[14] R. Werner, "The gravitational potential of a homogeneous polyhedron or don't cut corners," *Celestial Mechanics and Dynamical Astronomy*, Vol. 59, Jul 1994, 10.1007/BF00692875.

[15] R. A. Werner and D. J. Scheeres, "Exterior gravitation of a polyhedron derived and compared with harmonic and mascon gravitation representations of asteroid 4769 Castalia," *Celestial Mechanics and Dynamical Astronomy*, Vol. 65, No. 3, 1996, pp. 313–344, 10.1007/BF00053511.

[16] Y. Yu and H. Baoyin, "Generating families of 3D periodic orbits about asteroids," *Monthly Notices of the Royal Astronomical Society*, Vol. 427, 11 2012, pp. 872–881, 10.1111/j.1365-2966.2012.21963.x.

[17] Y. Jiang, H. Baoyin, and H. Li, "Periodic motion near the surface of asteroids," *Astrophysics and Space Science*, Vol. 360, 2015, https://doi.org/10.1007/s10509-015-2576-0.

[18] Y. Jiang, J. Schmidt, H. Li, X. Liu, and Y. Yang, "Stable periodic orbits for spacecraft around minor celestial bodies," *Astrodynamics*, Vol. 2, 2018, 10.1007/s42064-017-0014-5.

[19] Y. Jiang and X. Liu, "Equilibria and orbits around asteroid using the polyhedral model," *New Astronomy*, Vol. 69, 2019, pp. 8–20, https://doi.org/10.1016/j.newast.2018.11.007.

[20] T. Detroux, L. Renson, L. Masset, and G. Kerschen, "The harmonic balance method for bifurcation analysis of large-scale nonlinear mechanical systems," *Computer Methods in Applied Mechanics and Engineering*, Vol. 296, nov 2015, pp. 18–38, 10.1016/j.cma.2015.07.017.

[21] E. Petrov, "Analytical formulation of friction interface elements for analysis of nonlinear multi-harmonic vibrations of bladed disks," *Journal of Turbomachinery*, Vol. 125, 02 2003, pp. 364–371.

[22] G. Hill, "On the part of the motion of the lunar perigee which is a function of the mean motions of the sun and moon," *Acta Mathematica*, Vol. 8, 1886, pp. 1–36, 10.1007/BF02417081.

[23] L. Xie, S. Baguet, B. Prabel, and R. Dufour, "Bifurcation tracking by Harmonic Balance Method for performance tuning of nonlinear dynamical systems," *Mechanical Systems and Signal Processing*, Vol. 88, May 2017, pp. 445–461, 10.1016/j.ymssp.2016.09.037.

[24] R. Pusenjak and M. Oblak, "Incremental harmonic balance method with multiple time variables for dynamical systems with cubic non-linearities," *Numerical method in engineering*, Vol. 59, 2003, pp. 255–292, https://doi.org/10.1002/nme.875.

[25] M. Guskov and T. F., "Harmonic Balance-Based Approach for Quasi-Periodic Motions and Stability Analysis.," *Journal of Vibration and Acoustics*, Vol. 134, June 2012, 10.1115/1.4005823.

[26] *Non-Linear Vibrations of Multi-Stage Bladed Disks Systems With Friction Ring Dampers*, Vol. Volume 5: 6th International Conference on Multibody Systems, Nonlinear Dynamics, and Control, Parts A, B, and C of *International Design Engineering Technical Conferences and Computers and Information in Engineering Conference*, 09 2007, 10.1115/DETC2007-34473.

[27] N. Leclère, G. Kerschen, and L. Dell'Elce, "Multiple bifurcations around 433 Eros with Harmonic Balance Method," *Proceedings of the International Astronomical Union*, Vol. 15, No. S364, 2019, p. 171–177, 10.1017/S1743921322000734.

[28] Z. Musielak and B. Quarles, "The three-body problem," *Reports on Progress in Physics*, Vol. 77, Jun 2014, 10.1088/0034-4885/77/6/065901.

[29] A. Celletti and A. Giorgilli, "On the stability of the lagrangian points in the spatial restricted problem of three bodies," *Celestial Mechanics and Dynamical Astronomy*, Vol. 50, March 1990, 10.1007/BF00048985.

[30] V. Jeaumouillé, S. J.J., and P. B., "An adaptive harmonic balance method for predicting the nonlinear dynamic responses of mechanical systems–Application to bolted structures.," *Journal of Sound and Vibration*, Vol. 329, Sep 2012, 10.1016/j.jsv.2010.04.008.

[31] R. Seydel, *Practical bifurcation and stability analysis.* Springer-Verlag, 2010.

[32] L. Peletan, S. Baguet, M. Torkhani, and G. Jacquet-Richardet, "A comparison of stability computational methods for periodic solution of nonlinear problems with application to rotordynamics," *Nonlinear Dynamics*, Vol. 72, No. 3, 2013, pp. 671–682, 10.1007/s11071-012-0744-0.

[33] G. Von Groll and D. Ewins, "THE HARMONIC BALANCE METHOD WITH ARC-LENGTH CONTINUATION IN ROTOR/STATOR CONTACT PROBLEMS," *Journal of Sound and Vibration*, Vol. 241, No. 2, 2001, pp. 223–233, https://doi.org/10.1006/jsvi.2000.3298.

[34] G. Moore, "Floquet Theory as a Computational Tool," *SIAM Journal on Numerical Analysis*, Vol. 42, No. 6, 2005, pp. 2522–2568.

[35] J. Wu, L. Hong, and J. Jiang, "A robust and efficient stability analysis of periodic solutions based on harmonic balance method and Floquet-Hill formulation," *Mechanical Systems and Signal Processing*, Vol. 173, 2022, p. 109057, https://doi.org/10.1016/j.ymssp.2022.109057.

[36] B. Meini, "A "shift-and-deflate" technique for quadratic matrix polynomials," *Linear Algebra and its Applications*, Vol. 438, No. 4, 2013, pp. 1946–1961. 16th ILAS Conference Proceedings, Pisa 2010, https://doi.org/10.1016/j.laa.2011.11.037.

[37] Y. Ni, Y. Jiang, and H. Baoyin, "Multiple bifurcations in the periodic orbit around Eros," *Astrophysics and Space Science*, Vol. 361, 2016, pp. 1–15.

[38] Y. Jiang, H. Baoyin, and Y. Yu, "Topological Classifications and Bifurcations of Periodic Orbits in the Potential Field of Highly Irregular-shaped Celestial Bodies," *Nonlinear Dynamics*, Vol. 81, 2015.

[39] R. Seydel, "Practical bifurcation and stability analysis," *Springer Science Business Media*, Vol. 5, 2009.

[40] H. Kang, Y. Jiang, and H. Li, "Pseudo bifurcation and variety of periodic ratio for periodic orbit families close to asteroid (22) Kalliope," *Planetary and Space Science*, Vol. 158, 2018, pp. 69–86, https://doi.org/10.1016/j.pss.2018.05.002.

PERIOIDIC ORBITS AROUND 433 EROS

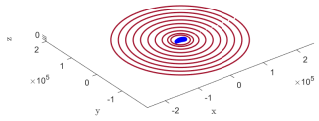

(a)

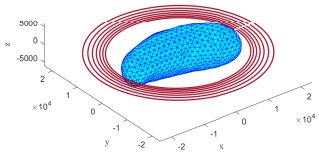

(b)

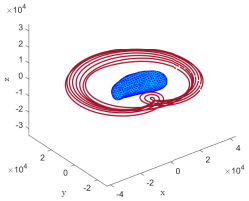

(c)

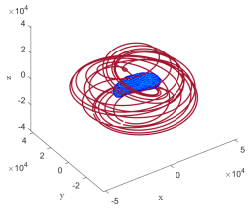

(d)

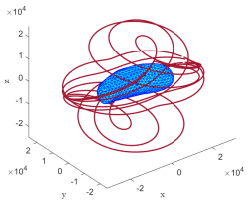

(e)

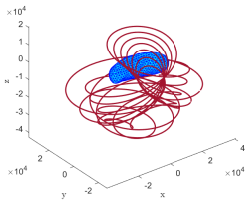

(f)

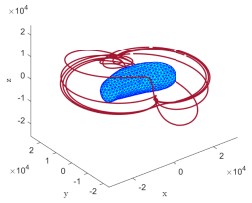

(g)

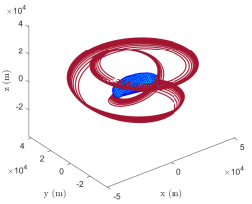

(h)

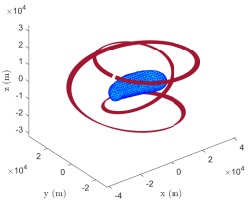

(i)

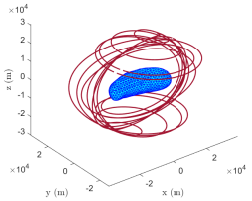

(j)

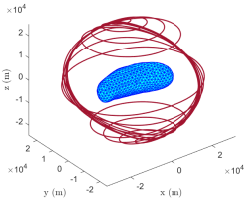

(k)

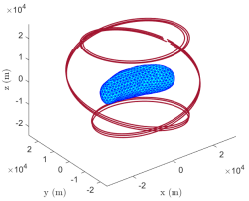

(l)

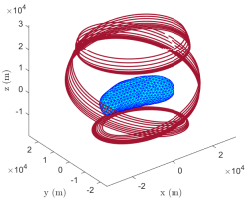

(m)

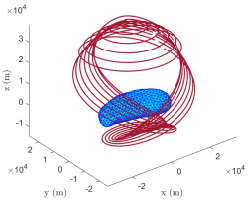

(n)

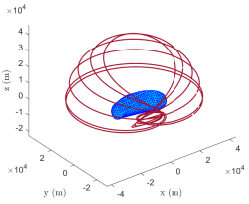

(o)

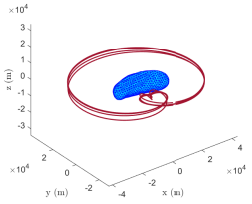

(p)

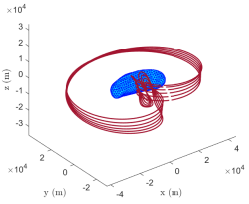

(q)